Journal of Catalysis **203,** 242–252 (2001)
doi:10.1006/jcat.2001.3329, available online at http://www.idealibrary.com on IDEAL®

Effect of Mg and Zr Modification on the Activity of VO_x/Al_2O_3 Catalysts in the Dehydrogenation of Butanes

M. E. Harlin,*,[1] V. M. Niemi,* A. O. I. Krause,† and B. M. Weckhuysen‡

*Fortum Oil and Gas Oy, P.O. Box 310, FIN-06101 Porvoo, Finland; †Helsinki University of Technology, Industrial Chemistry, P.O. Box 6100, FIN-02015 HUT, Finland; and ‡Departement Anorganische Chemie en Katalyse, Debye Instituut, Universiteit Utrecht, Sorbonnelaan 16, P.O. Box 80083, NL-3508 TB Utrecht, The Netherlands

Received April 12, 2001; revised June 15, 2001; accepted July 2, 2001

The initial activity of alumina-supported vanadium oxide catalysts with and without Mg and Zr was studied in the dehydrogenation of *i*-butane and *n*-butane at 580°C under atmospheric pressure. The catalyst activity was evaluated, after reduction with H_2 and CO, as a function of the amount of the promotor. The dehydrogenation activity was highest after CO reduction, and the selectivity toward *i*-butene increased and the formation of coke decreased with the addition of Mg. According to X-ray photoelectron spectroscopy, electron spin resonance, temperature programmed reduction, and Fourier transform infrared measurements, during CO reduction, V^{3+} species and two kinds of V^{4+} species with different coordinations (A and B) were formed on the catalyst surface. During H_2 reduction V^{3+} and some V^{4+} (B) species were formed. Apparently both V^{4+} and V^{3+} species were active in the dehydrogenation, and tentatively, we conclude that the activity of V^{4+} (A) was higher than that of V^{3+}. For the modified and unmodified catalysts, the oxidation states after reduction, both with H_2 and with CO, were similar and were not the main reason for the differences in activities. It is likely that the differences in activities induced by the promotors were due to the acidities of the catalysts, which had an influence on the side reactions of cracking, skeletal isomerization, and coke formation. The oxidative dehydrogenation during the first minutes on butane stream with calcined catalysts was also affected by the acidity of the catalyst. © 2001 Academic Press

Key Words: **supported vanadium oxides; dehydrogenation; butane; promotors; spectroscopy.**

INTRODUCTION

The dehydrogenation of light alkanes to the corresponding alkenes is commercially carried out with supported chromium oxide catalysts (1, 2) and platinum metal catalysts (3, 4). Other, noncommercial alkane dehydrogenation catalysts are based on Mo (5–10), V (11–15), Pd (16), Zn (17, 18), Ni (19), and Ga (20). Supported vanadium oxide catalysts have mainly been studied, however, for the oxidative dehydrogenation of alkanes resulting in the formation of alkenes and water (21–24). This reaction proceeds via the Mars–van Krevelen mechanism and V^{5+} species have been proposed as the active sites (25–27). Alkane molecules react with oxygen atoms and the reduced vanadium cations that are formed are reoxidized in the oxidative atmosphere. In earlier work (11), we showed that supported vanadium oxide catalyst is also active in the dehydrogenation of alkanes in the absence of oxygen, and the main products are then alkenes and hydrogen. The catalytic performance of VO_x/Al_2O_3 was investigated after pretreatment with H_2, CH_4, and CO, and the highest activity was obtained after CO reduction. Reduced V^{4+} or V^{3+} centers, or both, were proposed as the active dehydrogenation sites.

The goal of this work was to study the influence of promotors Mg and Zr on the catalytic performance of supported vanadium oxide. Promotors, and in particular alkali metal ions, are known to influence the redox and acid–base properties of vanadium oxide catalysts (21, 28, 29). This means that the addition of Mg or Zr to a VO_x/Al_2O_3 catalyst may have an effect on the catalytic performance in alkane dehydrogenation reactions in the absence of oxygen. The activity of supported vanadium oxide, with and without a promotor, was studied here as a function of reaction time and the catalyst pretreatment. The oxidation states of vanadium were studied by electron spin resonance (ESR), temperature programmed reduction (TPR), and X-ray photoelectron spectroscopy (XPS) and their influence on the catalyst activity and selectivity is discussed.

EXPERIMENTAL

1. Catalyst Preparation

Supported vanadium oxide catalysts were prepared by the incipient wetness impregnation method with alumina as the support. Before impregnation, the alumina support (Akzo Nobel 000-1.5E) was crushed and sieved to a particle size of 0.3–0.5 mm and calcined at 750°C for 16 h with 5% oxygen in nitrogen (Aga; O_2, 99.998%; N_2,

[1] To whom correspondence should be addressed. Fax: +358 10 45 27072. E-mail: elina.harlin@fortum.com.

0021-9517/01 $35.00
Copyright © 2001 by Academic Press
All rights of reproduction in any form reserved.

99.999%). The impregnation was accomplished by dissolving NH_4VO_3 (Merck, >99%) in an aqueous solution of oxalic acid (Riedel-de Haën AG, >99.5%). After impregnation the catalyst was dried at 120°C for 8 h and calcined at 700°C for 2 h with 5% O_2 in N_2. When promotor (Mg or Zr) was used it was impregnated before the vanadium by applying an aqueous solution of magnesium nitrate $Mg(NO_3)_2 \cdot 6H_2O$ (Merck, >99%) or $ZrO(NO_3)_2 \cdot 7H_2O$ (Aldrich, reagent grade). The drying and calcination steps were carried out in the same way as for vanadium impregnation.

2. Activity Measurements

The activity measurements were carried out at 580°C under atmospheric pressure in a fixed-bed microreactor. The catalyst (load of 0.2 g) was heated to the reaction temperature under 5% oxygen flow (Aga; O_2, 99.5%, N_2, 99.999%). The *n*-butane (Aga, 99.95%) or *i*-butane feed (Aga, 99.95%) with a weight hourly space velocity (WHSV) of 5 h^{-1} was diluted with nitrogen (Aga, 99.999%), the molar ratio of nitrogen to butane being 9 : 1. The nitrogen was purified with an Oxisorb (Messer Griesheim). The activity of the catalyst was followed for 15 min, after which the catalyst was flushed with nitrogen and regenerated with diluted air. Several cycles were performed with the same catalyst. Some of the catalysts were reduced with 5% H_2 (Aga, 99.999%) or 5% CO (Messer Griesheim GmbH, 99.997%) in N_2 for 30 min at 585°C before the activity measurements.

The products were analyzed on-line with a Fourier transform infrared (FTIR) gas analyzer (Gasmet, Temet Instruments Ltd.). The FTIR spectra were measured in the wavenumber range 850–4000 cm^{-1} with a resolution of 8 cm^{-1} at a scanning rate of 10 scans/s. The cuvette (9 cm^3) was maintained at constant temperature (175°C) and pressure (103 kPa). The method of analyzing the reaction products by FTIR gas analysis has been discussed in detail elsewhere (30). During the first minute on stream, the spectra were measured every 3 s; then they were measured every 7 s, and after a few minutes every 30 s.

The hydrocarbons formed during the dehydrogenation were also analyzed on-line with a gas chromatograph (GC) HP 6890 after 10 min on stream. A capillary column (HP-Plot/Al_2O_3 "M" deactivated) and a flame ionization detector were used to separate and detect the hydrocarbons. After the GC sampling, the analysis with the FTIR gas analyzer was continued. The lines to the FTIR gas analyzer and the GC were heated to 175°C. The conversion and selectivities were calculated from the reactor product on the basis of the carbon balance. The calculation is presented in detail elsewhere (5). The coke formed on the catalyst during the dehydrogenation was not taken into account in the carbon balance.

3. Catalyst Characterization

After dissolution of the solids, the amounts of V and Mg were measured by atomic absorption spectroscopy (AAS) and the amount of Zr was measured by inductively coupled plasma (ICP). The surface area of the catalyst was determined with a Coulter Omnisorp 100CX (static volumetric method). The crystalline structure was studied by X-ray diffraction (XRD) analysis with a Siemens D500 instrument using Cu$K\alpha$ radiation. The reduction of the catalysts was studied by TPR. The measurements were performed with an Altamira Instruments AMI-100 catalyst characterization system. Catalyst samples (50 mg) were dried at 130°C for 60 min with helium, calcined with 5% O_2/He at 600°C for 30 min, and cooled down to 30°C in air. The samples were then heated from 30°C to 580 or 750°C at a rate of 5°C/min under 10% H_2 in argon (30 cm^3/min) and kept at the final temperature for 30 min. The consumption of hydrogen was measured with a thermal conductivity detector.

Some of the catalysts were investigated with XPS. For this purpose, the catalysts were heated to 580–585°C under 5% oxygen flow in the fixed-bed microreactor and some of the catalysts were then reduced with 5% H_2 or 5% CO in N_2 for 30 min. After this, the catalysts were inertly transferred to a glove box and prepared for analysis under nitrogen atmosphere. Finally, they were transferred to the XPS instrument under vacuum. The XPS measurements were performed in an X-probe Model 101 spectrometer (Surface Science Instruments, VG Fisons) using a monochromatized Al$K\alpha$ X-ray source. A nickel grid and a flood gun were used to compensate for sample charging. The background pressure during the XPS acquisition was better than 1×10^{-6} Pa (1×10^{-8} Torr). High-resolution spectra of the V 2*p*, Mg 2*s*, Zr 3*d*, Al 2*p*, O 1*s*, and C 1*s* regions with a resolution of 0.9 eV and a low-resolution survey spectrum were measured using a nominal spot size of 600 μm. Atomic sensitivity factors provided by the instrument manufacturer were used to calculate the relative surface concentrations. The Al 2*p* line (74.5 eV) was used as a binding energy reference. The overlapping signals were deconvoluted using symmetrical Gaussian–Lorenzian (80/20) lines with the following constraints for all oxidation states: nonlinear Shirley background subtraction, an intensity ratio of V2$p_{3/2}$ to V2$p_{1/2}$ of 2.19; and a doublet separation (V2$p_{1/2}$–V2$p_{3/2}$) of 7.3–7.6 eV. The oxidation state and coordination environment of the supported vanadium oxide catalysts after different treatments were also measured by ESR. The ESR spectra were taken with a Bruker ESP300E spectrometer equipped with a double rectangular TE_{104} mode cavity in *X* band at −153 and 27°C. Selected ESR spectra were simulated with the SIMPOW program, which generates a powder spectrum calculated to second order. A linear background subtraction was applied for each ESR spectrum by using

the Bruker ESP300E spectrometer (within the range 0 to 6800 G). Quantitative ESR measurements of V^{4+} were performed by double integration of the spectra and comparison with a $Cu(acac)_2$/KCl reference sample with known spin density.

RESULTS

1. Characterization of Fresh Catalysts

The vanadium and promotor contents of the supported vanadium oxide catalysts are presented in Table 1. For all the catalysts the vanadium content was between 4 and 6 wt%, while the amounts of Mg and Zr varied. The sample designations given in Table 1 indicate the measured amounts of vanadium and promotor in the catalyst. The XRD pattern of the V5 catalyst showed reflections typical for the alumina support. Since the pattern of crystalline vanadium oxide was not detected, we assume that the vanadium oxide was well dispersed in the catalyst. The XRD patterns of the catalysts V5Mg2 and V5Mg5 only showed reflections for the alumina support, but the presence of mixed Mg–Al–O was indicated by the shift of the reflections from γ-alumina toward smaller 2θ angles, i.e., larger d spacing and by the change in the intensity ratios. In addition, the catalyst V5Mg9 also showed some reflections at 43° 2θ and 62° 2θ, indicating the presence of MgO crystallites. The XRD diffractograms do not exclude the possibility of Mg vanadates, however, since their crystal size could be below the detection limit of the method (31–33). The zirconium-modified catalysts contained two crystal forms of ZrO_2: monoclinic and tetragonal. The content of crystalline ZrO_2 in V6Zr12 was higher than that in V5Zr5. Some small diffraction peaks indicated the presence of a minor amount of ZrV_2O_7 as well. This is in line with Khodakov *et al.* (34), who observed the conversion of ZrO_2 to the monoclinic phase and the formation of ZrV_2O_7 after they calcined the VO_x/ZrO_2 catalyst at temperatures above 600°C. The reflections from the support were not shifted like for the Mg-modified catalysts. The crystalline size, as calculated from the half-width of the diffraction peak from γ-alumina (4,4,0) using the Scherrer equation was 58 ± 2 Å for all the catalysts. Finally, the BET surface areas of the catalysts are comparable with the BET surface area of the alumina support treated under identical conditions. This supports the conclusion that the species impregnated on alumina were well dispersed.

2. Catalytic Activity Measurements

The thermal reactions of butanes were studied in the absence of catalyst by replacing the catalyst material with carborundum of equal volume. Under the conditions used for the activity tests, the conversions of *i*-butane and *n*-butane were below 2%. The activity of the unmodified V5 catalyst was studied with *i*-butane feed at 580°C. Activities were studied after calcination of the catalyst and after reduction at 580°C for 30 min with H_2 or CO. The conversion of *i*-butane and the selectivity to *i*-butene after these pretreatments are presented in Fig. 1. The product composition was measured on-line with the FTIR gas analyzer during the first 7 min on stream, with the on-line gas chromatograph after 10 min on stream, and then again with the FTIR gas analyzer. The conversions and selectivities after 1 min on stream and the amounts of coke formed during the dehydrogenation test of 15 min are summarized in Table 2. As can be seen, the conversion of *i*-butane was highest after CO reduction. However, the activity declined rapidly. The conversion was lowest for the calcined vanadium oxide catalyst, but it increased slightly during the first minutes on stream. The selectivity to *i*-butene was the highest after CO reduction and the lowest after H_2 reduction. The activity pattern of the unmodified catalyst used as reference material has been presented in detail elsewhere (11). At 580°C

TABLE 1

Properties of the Catalysts

	V (wt%)	Mg (wt%)	Zr (wt%)	Mg/V (mol/mol)	Zr/V (mol/mol)	BET ($m^2/g_{catalyst}$)	Phases detected by XRD
Al_2O_3[a]	—	—	—	—	—	181	γ-Al_2O_3
V5	5.2	—	—	—	—	165	γ-Al_2O_3
V5Mg2	4.7	2.3	—	1.0	—	171	γ-Al_2O_3
V5Mg5	4.9	4.7	—	2.0	—	162	γ-Al_2O_3
V5Mg9	4.6	9.1	—	4.1	—	161	γ-Al_2O_3 MgO
V5Zr5	5.4	—	4.5	—	0.5	169	γ-Al_2O_3 ZrO_2 ZrV_2O_7
V6Zr12	5.9	—	11.6	—	1.1	127	γ-Al_2O_3 ZrO_2 ZrV_2O_7

[a] Calcined at 750°C for 16 h.

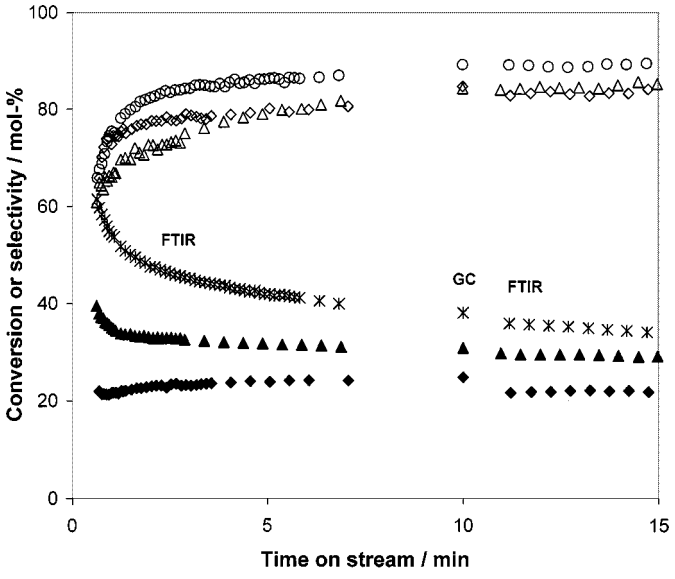

FIG. 1. Conversion of *i*-butane and selectivity to *i*-butene with calcined, H_2-reduced, and CO-reduced V5 catalysts. (◆) Conversion (calcined V5), (◇) selectivity to *i*-butene (calcined V5), (▲) conversion (H_2-reduced V5), (△) selectivity to *i*-butene (H_2-reduced V5), (∗) conversion (CO-reduced V5), (◯) selectivity to *i*-butene (CO-reduced V5).

and 1 bar with *i*-butane/nitrogen feed of 1:9 mol/mol, the thermodynamic equilibrium conversion of *i*-butane to *i*-butene and H_2 is 89%.

2.1. Dehydrogenation activity of Mg-modified VO_x catalysts. The conversions of *i*-butane and the selectivities to *i*-butene for Mg-modified catalyst V5Mg5 are shown in Fig. 2. The conversion of *i*-butane was higher after CO reduction than after calcining and H_2 reduction. The same result was obtained for the supported vanadium oxide catalysts in the absence of promotor, as noted above. The conversion was lower, however, and the selectivity to *i*-butene was higher than that for the catalysts without modification. Furthermore, the selectivities toward *i*-butene increased and the *i*-butane conversion decreased with higher contents of Mg. Table 2 indicates that the selectivities toward C_1–C_3 products, *n*-butenes, and 1,3-butadiene were lower with the Mg-modified VO_x catalyst than with the V5 catalyst. Neither H_2 nor CO reduction increased the selectivity for the formation of *n*-butenes and 1,3-butadiene. Finally, the amount of coke formation during the dehydrogenation tests with the calcined catalysts was lower for the Mg-modified material.

TABLE 2

Conversions of *i*-Butane and Selectivities after 1 min on Stream and the Amounts of Coke Formed during Tests of 15 min with Catalysts Pretreated in Different Ways

Catalyst pretreatment	Conversion of *i*-butane (%)	Selectivity to						Coke (mol/g_{cat})
		i-Butene (%)	*n*-Butenes and 1,3-butadiene (%)	C_1–C_3 (%)	*n*-Butane (%)	Heavier (%)	CO_x (%)	
			V5					
Calcination	22	74	8	9	4	3	3	9×10^{-4}
H_2 reduced	35	66	22	9	0	2	0	11×10^{-4}
CO reduced	54	75	14	8	1	2	0	18×10^{-4}
			V5Mg2					
Calcination	18	83	2	7	0	3	5	4×10^{-4}
H_2 reduced	29	91	4	4	1	0	0	12×10^{-4}
CO reduced	52	84	9	6	0	0	0	18×10^{-4}
			V5Mg5					
Calcination	19	83	3	5	1	2	4	4×10^{-4}
H_2 reduced	29	92	3	3	2	0	0	10×10^{-4}
CO reduced	44	90	5	4	1	0	0	16×10^{-4}
			V5Mg9					
Calcination	19	83	3	6	0	2	5	4×10^{-4}
H_2 reduced	26	92	1	5	1	1	0	10×10^{-4}
CO reduced	43	91	4	4	1	0	0	13×10^{-4}
			V5Zr5					
Calcination	24	76	11	7	0	3	3	13×10^{-4}
H_2 reduced	41	72	18	8	1	1	0	14×10^{-4}
CO reduced	54	77	14	7	1	1	0	21×10^{-4}
			V6Zr12					
Calcination	24	81	5	7	0	2	4	10×10^{-4}
H_2 reduced	39	81	13	5	0	1	0	12×10^{-4}
CO reduced	51	82	11	5	1	0	0	17×10^{-4}

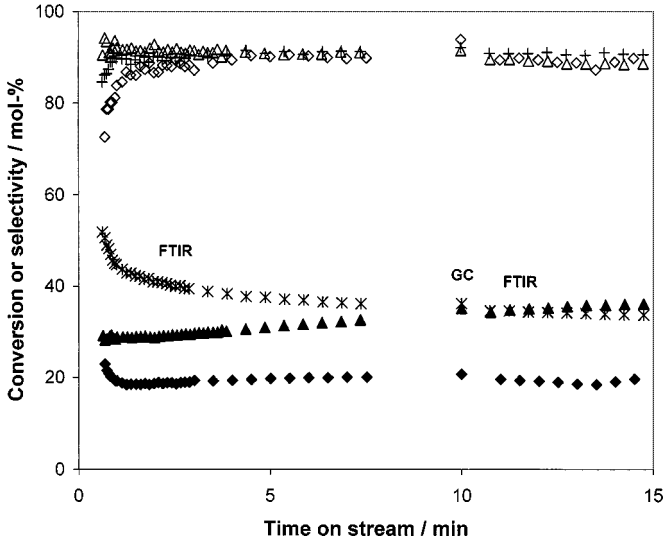

FIG. 2. Conversion of *i*-butane and selectivity to *i*-butene with calcined, H_2-reduced, and CO-reduced V5Mg5 catalysts. (◆) Conversion (calcined V5Mg5), (◇) selectivity to *i*-butene (calcined V5Mg5), (▲) conversion (H_2-reduced V5Mg5), (△) selectivity to *i*-butene (H_2-reduced V5Mg5), (∗) conversion (CO-reduced V5Mg5), (+) selectivity to *i*-butene (CO-reduced V5Mg5).

2.2. Dehydrogenation activity of Zr-modified VO_x catalysts. As shown in Fig. 3, the calcined and H_2-reduced Zr-modified VO_x catalyst V5Zr5 showed slightly higher activity and selectivity to *i*-butene than the catalyst without modification. However, after CO reduction the conversion and selectivities obtained with catalysts V5 and V5Zr5 were very similar. The amount of coke formed during the dehydrogenation test of 15 min was also similar for catalysts V5 and V5Zr5, as summarized in Table 2.

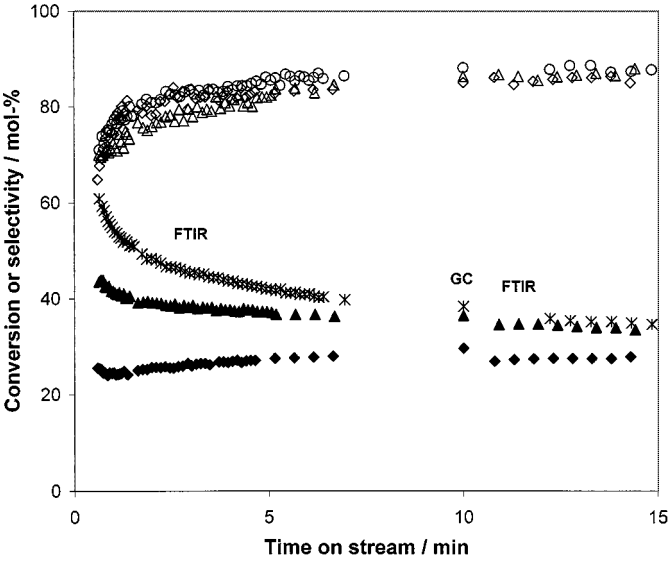

FIG. 3. Conversion of *i*-butane and selectivity to *i*-butene with calcined, H_2-reduced, and CO-reduced V5Zr5 catalysts. (◆) Conversion (calcined V5Zr5), (◇) selectivity (calcined V5Zr5), (▲) conversion (H_2-reduced V5Zr5), (△) selectivity (H_2-reduced V5Zr5), (∗) conversion (CO-reduced V5Zr5), (◯) selectivity (CO-reduced V5Zr5).

2.3. Effect of water treatment on catalyst performance. It was observed in our previous study (11) that the adsorption of water on the catalyst surface prior to the activity test noticeably affects the catalyst activity. We now continue those experiments. The calcined catalyst V5 was treated with a feed containing nitrogen and 3% water for 3 min, and after calcination and water treatment the activity of the catalyst was measured in the dehydrogenation of *i*-butane. The conversion of *i*-butane and the selectivities were identical to those presented in Fig. 1. Apparently the water treatment has no effect on the activity of the calcined catalyst, which mainly consists of V^{5+} species.

The same water pretreatment was performed after H_2 and CO reduction: the catalyst was reduced with H_2 or CO for 30 min and then treated with 3% H_2O in N_2 stream for 3 min. After this, the activity of the catalyst was measured in the dehydrogenation of *i*-butane. The conversion of *i*-butane was stable at 30% for 15 min after both H_2 and CO reduction. In the absence of water treatment, the initial conversion of *i*-butane was 60% after CO reduction and 40% after H_2 reduction (see Fig. 1). Thus, H_2O appears to deactivate the catalytically active $V^{3+/4+}$ species formed during the prereduction step. However, no CO_x compounds were formed during the *i*-butane test after water treatment. A similar decrease in the activity was observed for the Mg- and Zr-modified catalysts.

2.4. Dehydrogenation activity with n-butane feed. The results of the dehydrogenation tests performed with the *n*-butane feed and V5 catalysts are presented in Fig. 4. The conversions of *n*-butane and the selectivities of *n*-butenes and 1,3-butadiene are presented for calcined, CO-reduced, and H_2-reduced catalysts. The conversion and selectivities show trends similar to those of the *i*-butane test. The highest activity was obtained after reduction with CO, the conversion of *n*-butane being 45% after 1 min on *n*-butane stream. The decrease in the conversion of *n*-butane was faster, however, and the coke formation was slightly higher than that during the *i*-butane feed (Table 3). The total selectivity to unsaturated C_4 products was similar with the *n*-butane and *i*-butane feeds. However, the selectivity for the formation of *i*-butene with the *n*-butane feed was clearly lower than the selectivity for the formation of *n*-butenes and 1,3-butadiene with the *i*-butane feed. The results obtained with catalysts V5Mg5 and V5Zr5 after 1 min on stream are shown in Table 3. The selectivities for the formation of lighter and heavier hydrocarbons were higher with the *n*-butane feed than with the *i*-butane feed.

In addition to the activity, the acid–base character of the catalyst can influence the distribution of *n*-butenes in the product (21). The distributions of 1-butene, *cis*-2-butene, *trans*-2-butene, and 1,3-butadiene, expressed relative to the amount of *cis*-2-butene, were 0.6/1.0/1.2/2.3 for V5,

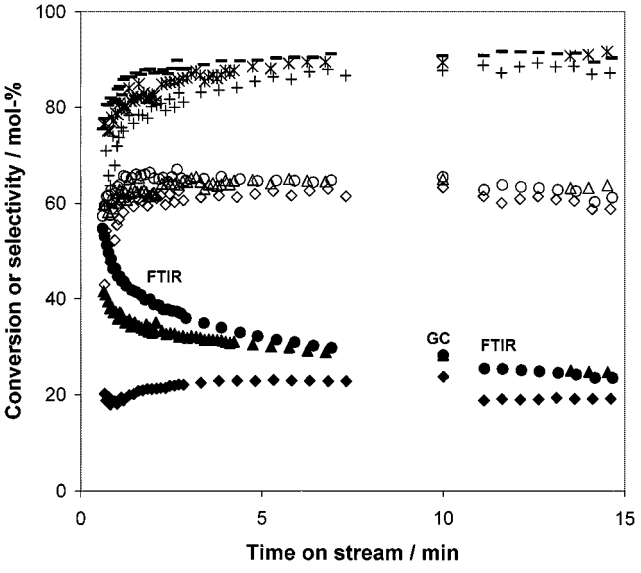

FIG. 4. The conversion of *n*-butane and selectivities to *n*-butenes and 1,3-butadiene with calcined, H_2-reduced, and CO-reduced V5 catalysts. (◆) Conversion of *n*-butane (calcined), (◇) selectivity of *n*-butenes (calcined), (+) selectivity to *n*-butenes and butadiene (calcined), (▲) conversion of *n*-butane (H_2-reduced), (△) selectivity to *n*-butenes (H_2-reduced), (∗) selectivity to *n*-butenes and butadiene (H_2-reduced), (●) conversion of *n*-butane (CO-reduced), (○) selectivity to *n*-butenes (CO-reduced), (—) selectivity to *n*-butenes and butadiene (CO-reduced).

1.0/1.0/1.1/4.6 for V5Mg5, and 1.0/1.0/1.2/3.3 for V5Zr5 after 0.5 min on *n*-butane stream. Thus, the fraction of 1,3-butadiene was high during the first minute on stream with all three catalysts and highest with the Mg-modified catalyst. In all cases, however, it rapidly decreased near the ratio 1/1. After H_2 and CO reductions of the catalysts, the distribution was stable and close to 1/1/1/1 during the test of 15 min, similar to the situation prevailing after several minutes on *n*-butane stream with the untreated catalysts. Under the test conditions at thermodynamic equilibrium the conversion of *n*-butane to 1-butene, *cis*-2-butene, *trans*-2-butene, 1,3-butadiene, and H_2 is 88% and the distribution of the *n*-butenes and 1,3-butadiene listed above is 0.9/1.0/1.4/1.1.

TABLE 4

Reduction of Catalysts Measured with the On-Line FTIR Gas Analyzer

	O/V (mol/mol)	AOS of V[a]
V5		
H_2 reduction	0.61	3.6
CO reduction	0.71	4.0
V5Mg5		
H_2 reduction	0.41	4.0
CO reduction	0.76	4.0
V5Zr5		
H_2 reduction	0.71	3.4
CO reduction	0.76	3.8

[a] AOS, average oxidation state. Estimates of water retention and Boudouard reaction are included.

3. Reduction Experiments and Catalyst Characterization

During the reductions with H_2 or CO, prior to the activity tests, the amounts of evolved water and CO_2 were measured with an on-line FTIR gas analyzer. The reduction is presented in Table 4 as the molar ratio of the amount of released oxygen to the amount of vanadium (O/V). After taking into account the Boudouard reaction during CO reduction and the estimate of the water retainment during H_2 reduction (11), we calculated the average oxidation states for vanadium after H_2 and CO reduction as between 3.4 and 4.

TABLE 3

Conversions of *n*-Butane and Selectivities after 1 min on Stream and the Amounts of Coke Formed during Tests of 15 min on Catalysts Pretreated in Different Ways

		Selectivity to						
Pretreatment	Conversion of *n*-butane (%)	*n*-Butenes and 1,3-butadiene (%)	*i*-Butene (%)	C_1–C_3 (%)	*i*-Butane (%)	Heavier (%)	CO_x (%)	Coke (mol/g_{cat})
			V5					
Calcination	18	71	4	17	0	3	5	13×10^{-4}
H_2 reduced	37	79	8	8	1	4	0	15×10^{-4}
CO reduced	45	83	4	9	0	3	0	22×10^{-4}
			V5Mg5					
Calcination	18	75	3	9	1	4	7	6×10^{-4}
H_2 reduced	26	89	2	7	1	1	0	20×10^{-4}
CO reduced	44	88	2	8	0	2	0	27×10^{-4}
			V5Zr5					
Calcination	18	61	9	18	1	6	5	13×10^{-4}
H_2 reduced	37	80	7	10	0	3	0	19×10^{-4}
CO reduced	47	83	5	9	0	3	0	26×10^{-4}

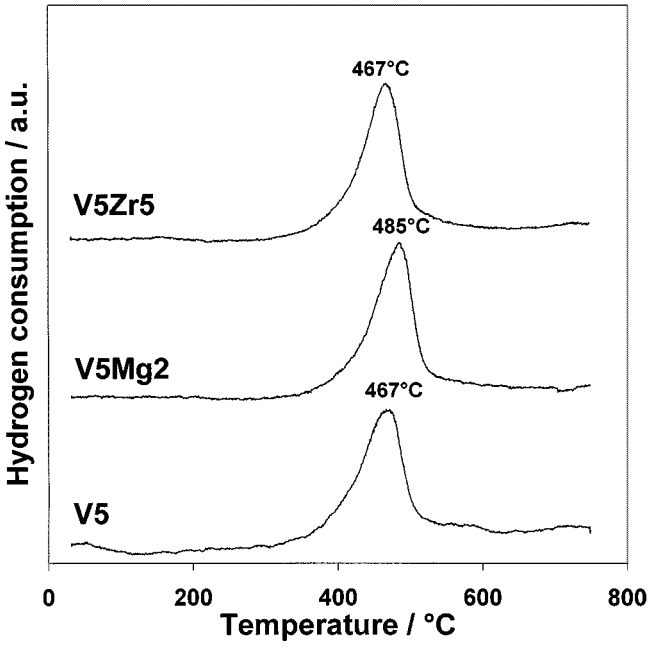

FIG. 5. TPR profiles of the V5, V5Mg2, and V5Zr5 catalysts.

The TPR measurements (presented in Fig. 5) show that the V5 and V5Zr5 catalysts were reduced at the same temperature, while the Mg-modified catalyst V5Mg2 was reduced at a temperature 20°C higher. The consumption of hydrogen (Table 5) was similar for the three catalysts. Assuming a reduction stoichiometry of 0.5 H_2/V from V^{5+} to V^{4+} and an average oxidation state of 5 for the calcined catalyst, the average oxidation state of vanadium in catalyst V5 would be 3.5 after reduction to 580°C.

The vanadium species present after H_2 and CO reduction were studied in more detail by XPS and ESR methods. The deconvolution of the XPS spectra of the V 2*p* region indicated the presence of three doublets, i.e., three oxidation states of vanadium. The line for V $2p_{3/2}$ was between 517.4 and 517.7 eV for V^{5+}, between 516.4 and 516.7 eV for V^{4+}, and between 515.8 and 516.1 eV for V^{3+}. A typical result of the peak-fitting procedure for V5 was presented earlier (11). The amount of each oxidation state was obtained after deconvolution of the spectra, and the average oxidation states of vanadium in the different catalysts are presented in Table 6. In the calcined V5 catalyst the vanadium oxide was in oxidation state 5+, but the calcined Mg- and Zr-modified catalysts also contained small amounts of oxidation states 4+ and 3+. Species V^{5+}, V^{4+}, and V^{3+} were observed after the H_2 and CO reductions. The line for Mg 2*s* was between 89.1 and 89.3 eV. The XPS results showed a molar ratio Mg/V of 1.0 for the calcined V5Mg2 catalyst. The line for Zr $3p_{5/2}$ was between 182.0 and 182.2 eV, and a molar ratio Zr/V of 0.5 was obtained for the calcined V5Zr5 catalyst.

Figure 6 shows the ESR spectra of the sample V5 after different treatments. All the spectra are typical for V^{4+}, with a d^1 configuration and a nuclear spin I of $\frac{7}{2}$, resulting in a complex spectrum with a large number of hyperfine lines. Detailed analysis of the spectra of the catalysts V5, V5Mg5, and V5Zr5 by spectrum simulation and quantitative determination of the spin concentration of V^{4+} reveals

TABLE 5

Consumption of H_2 during TPR Measurements from 30 to 580°C

	Maximum H_2 consumption	H_2 consumption (mol/g)	H_2/V	AOS of V[a]
V5	467°C	7.6×10^{-4}	0.75	3.5
V5Mg2	485°C	7.3×10^{-4}	0.79	3.4
V5Zr5	467°C	8.4×10^{-4}	0.80	3.4

[a] AOS, average oxidation state.

TABLE 6

Results of Peak Deconvolution of the V Photoelectron Signal after Calcination of the Catalyst with Air and after Reduction with H_2 or CO for 30 min at 580°C

Treatment	V^{5+}	V^{4+}	V^{3+}	AOS of V[a]	$\frac{V/Al}{V_{calcined}/Al_{calcined}}$
			V5		
Calcination	100%	—	—	+5.0	1
H_2 reduction	21%	37%	42%	+3.8	0.7
CO reduction	32%	41%	27%	+4.1	0.8
			V5Mg2		
Calcination	80%	11%	9%	+4.7	1
H_2 reduction	15%	4%	81%	+3.3	1.1
CO reduction	6%	54%	40%	+3.7	1.1
			V5Zr5		
Calcination	69%	14%	17%	+4.5	1
H_2 reduction	6%	30%	64%	+3.4	0.8
CO reduction	4%	37%	59%	+3.5	1.0

[a] AOS, average oxidation state.

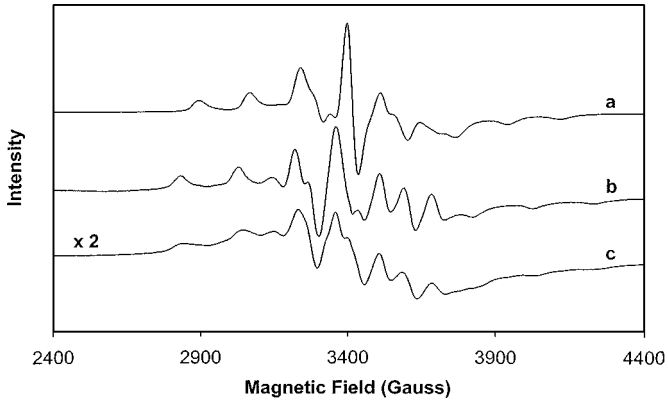

FIG. 6. ESR spectra of V5 measured at −153°C: (a) after calcination in oxygen at 580°C for 6 h, before measurement the sample was treated in He for 5 min at room temperature; (b) after reduction with hydrogen at 580°C for 30 min; and (c) after reduction with carbon monoxide at 580°C for 30 min.

TABLE 7

Quantitative Determination of V^{4+} by Double Integration of the ESR Spectra of the Supported Vanadium Oxide Catalysts

Pretreatment	V5 (%)	V5Mg5 (%)	V5Zr5 (%)
Calcination in O_2 at 580°C for 6 h	8	7	12
Reduction with H_2 at 580°C for 30 min	13	5	14
Reduction with CO at 580°C for 30 min	35	34	31

TABLE 8

Quantitative Determination of V^{4+} and the Relative Amounts of Species A and B for a V5Mg5 Catalyst after Different Pretreatments

Pretreatment	V^{4+} (%)	Species A (%)	Species B (%)
Calcination in O_2 at 580°C for 6 h	7	7	—
Reduction with CO at 200°C for 30 min	9	8	1
Reduction with CO at 300°C for 30 min	10	7	3
Reduction with CO at 400°C for 30 min	14	9	5
Reduction with CO at 500°C for 30 min	26	16	10
Reduction with CO at 580°C for 30 min	34	19	15

the following:

1. Two distinct magnetically isolated V^{4+} species were present, labeled as species A and B. The ESR parameters of the species were as follows: species A is characterized by $g_{xx} = g_{yy} = 1.984$, $g_{zz} = 1.946$, $A_{xx} = A_{yy} = 60$ G, and $A_{zz} = 172$ G, while species B is characterized by $g_{xx} = g_{yy} = 1.982$, $g_{zz} = 1.939$, $A_{xx} = A_{yy} = 75$ G, and $A_{zz} = 193$ G. These values are in agreement with those recently reported by Catana *et al.* (35).

2. Species A, which is the dominant species after calcination, was almost absent after reduction with hydrogen at 580°C, but a significant amount of species A was always present with CO as the reducing agent, even after reduction at 580°C.

3. The ESR spectrum was always broader and less resolved when CO was used as the reducing agent. This indicates that the paramagnetic species at the surface are close to each other, giving rise to spin–spin interactions.

4. The amounts of V^{4+} in the calcined and H_2- and CO-reduced catalysts were very similar for the three catalysts under study (Table 7), although the amounts varied significantly after the different pretreatments. Looking at the three catalysts together, the content of V^{4+} relative to the total V content was between 7 and 12% for the calcined catalyst, 5 and 14% for the H_2-reduced catalyst, and 31 and 35% for the CO-reduced catalyst. Thus, reduction with carbon monoxide leads to the highest concentrations of V^{4+} at the catalyst surface.

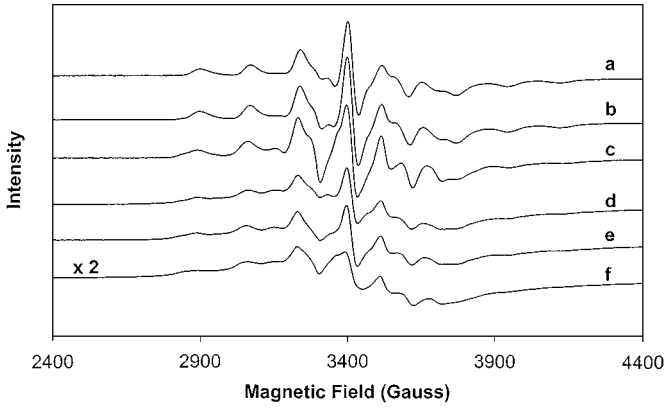

FIG. 7. Evolution of the ESR spectra of V5Mg5 measured at −153°C as a function of the reduction temperature: (a) after calcination in oxygen at 580°C for 6 h, before measurement the sample was treated in He for 5 min at room temperature; (b) after reduction with carbon monoxide at 200°C for 30 min; (c) after reduction with carbon monoxide at 300°C for 30 min; (d) after reduction with carbon monoxide at 400°C for 30 min; (e) after reduction with carbon monoxide at 500°C for 30 min; and (f) after reduction with carbon monoxide at 580°C for 30 min.

In another experiment we subjected the V5Mg5 catalyst to carbon monoxide reduction at different temperatures. The ESR spectra recorded after these treatments are shown in Fig. 7. The spectra indicate that the reduction with CO begins above 200°C and a new V^{4+} species B is generated at the catalyst surface. The amounts of V^{4+} and of species A and B in the V5Mg5 catalyst were obtained by spectrum simulation and double integration of the corresponding ESR spectra and the result of this quantitative analysis is given in Table 8. The results show that (1) after the reduction with carbon monoxide at 580°C the amount of V^{4+} is about 35% of the total V content (2), the amounts of species A and B increase with the reduction temperature, and (3) the amount of species A is always greater than the amount of species B at the catalyst surface, even at the highest reduction temperature. As was noted above, this last observation was not made for the samples reduced in hydrogen.

Finally, the V5Mg5 catalyst, first calcined and then treated in CO at 580°C, was subjected to a saturated N_2 stream of water at 580°C for 30 min. The ESR spectrum showed the presence of the two V^{4+} species A and B in almost the same ratio as after CO reduction. The only difference was a slight increase (3–5%) in the amount of V^{4+} in the catalyst material. This indicates that the same V^{4+} species are present in the catalyst before and after the water treatment.

DISCUSSION

1. Reduction of Catalysts

According to the XPS measurement the calcined vanadium oxide catalysts contained vanadium mostly in oxidation state 5+. This is in line with the ESR measurement,

which indicated only small amounts of V^{4+}, and with the observations of Wachs and Weckhuysen (36). The XRD indicated the incorporation of some Mg to the alumina matrix. Though the current XRD or ESR data did not indicate the incorporation of V into the matrix or the formation of magnesium vanadates, these processes can, however, occur as reported previously in the literature (31–33, 37).

The techniques we used in this study showed that the average oxidation states of the catalysts after CO and after H_2 reduction were similar. According to the TPR results, the Mg-modified catalyst reduces at a slightly higher temperature than the unmodified and the Zr-modified catalysts, indicating a more difficult reduction of the VO_x species. Still, after the reduction for 30 min at 580°C the average oxidation states of the three catalysts were fairly similar. The extent of the reduction of the vanadium species may decrease with increasing Mg content as shown by the higher average oxidation state obtained for catalyst V5Mg5 than for V5 (Table 4).

The ESR results were clearly different for the two reducing agents. The total amount of V^{4+} was highest after CO reduction, and two species of V^{4+} (A and B) were observed. The total amount of V^{4+} was quite small after H_2 reduction: evidently the vanadium was mainly reduced to oxidation state 3+ (38) and only a small amount of V^{4+} (B) was formed.

There were some discrepancies in the ESR and XPS results. The most significant discrepancies were between the amounts of V^{4+} calculated from the deconvoluted XPS spectra and measured by ESR after H_2 reduction of the unmodified and Zr-modified catalysts. Still, the trends with the two techniques were similar. The distribution of the V^{4+} and V^{3+} species is known to be highly dependent on the conditions of reduction (36). Some of the differences may also be accounted for by the specific features of the two techniques, for example, by background subtractions used for XPS and ESR.

From the TPR, XPS, FTIR, and ESR results together, we can conclude that, after reduction with H_2, the average oxidation state of vanadium was about 3.5. The oxidation states present were V^{5+}, V^{4+} (B), and V^{3+}. After CO reduction, the average oxidation state was slightly higher, about 3.9 owing to the greater amount of V^{4+} (A + B) and the smaller amount of V^{3+}. This indicates that vanadium oxide was reduced to lower state with H_2 than with CO. In this calculation it was assumed that the calcined catalyst contained only V^{5+} species. If, however, V^{4+} or V^{3+} species exist on the calcined catalyst, as indicated by the ESR and XPS measurements, the average oxidation state of the catalysts would be lower after the reductions. This would not influence the differences in the average oxidation states between the reducing agent used. It could, however, cause some difference when the average oxidation states of vanadium are compared between the various catalysts.

2. Activity

High activity of the alumina-supported vanadium oxide catalysts was obtained in the dehydrogenation of butanes to butenes and hydrogen. Activity was best with the CO-reduced catalyst, either unmodified or modified with Zr. The highest selectivity for the corresponding butene was obtained with the Mg-modified catalyst, however.

The characterizations of the reduced catalyst by ESR and XPS support the conclusion that the oxidation state V^{4+} or V^{3+} is the active phase in the dehydrogenation reaction. It is clear that the active phase was formed during the CO reduction. The vanadium species then present were V^{4+} (A and B) and V^{3+}. The activity may be reduced by 50% by adsorption of water on these sites. However, the ESR measurement showed that the water treatment did not affect the coordination of the V^{4+} sites. Moreover, no CO_x was released in the subsequent butane test. The activity of the catalysts was also high on the H_2-reduced surfaces, which contained mainly V^{3+} and V^{4+} (species B). Comparison of the results thus clearly shows that both V^{3+} and V^{4+} (A and/or B) are active in some degree. The activity of V^{4+} (A) is probably higher than that of V^{3+}.

The ESR and XPS studies also revealed that the oxidation state of the catalyst after reduction with H_2 or CO at 580°C was not different when the catalyst was modified with Mg and Zr. This means that the differences in the activities of the modified catalysts were not due to the different oxidation states of vanadium. Instead, they may have been due to changes in the hydrocarbon–catalyst interaction, which is proposed to be weaker on a catalyst of basic character (39, 40). A strong hydrocarbon–catalyst interaction is expected on an acid catalyst and this could lead to cracking and coke formation (highly dehydrogenated products), as observed in this study with the unmodified and Zr-modified vanadium oxide catalyst.

It can be assumed that the formation of *n*-butenes and 1,3-butadiene from the *i*-butane feed and of *i*-butene from the *n*-butane feed are due to consecutive dehydrogenation and isomerization reactions. The formation of isomerized products (skeletal isomerization) indicates higher acidity of the catalyst (41) and a bifunctional mechanism. With the V5 catalyst, the selectivity for isomerization increased markedly after reduction with H_2 or CO. Similar results were obtained with the Zr-modified catalyst. In the case of the Mg-modified catalyst the amount of isomerization was lower both after calcination and after H_2 and CO reductions, indicating a lower acidity.

Busca *et al.* (42) have reported that the reduced vanadium oxide should not be more acidic than the calcined oxide. The V/Al ratios measured by XPS for the reduced V5 and V5Zr5 catalysts were lower than those measured for the calcined catalysts (Table 6) and may indicate a poorer dispersion of the active phase on the alumina support. The higher acidity

of the reduced catalysts might then be due to the alumina support. The V/Al ratio was not decreased in the reduced Mg-modified catalyst, so in this case the dispersion of VO_x may not have been changed by the reduction and, therefore, the selectivity for skeletal isomerization remained lower. The better dispersion may have been due to the presence of Mg species.

The main side reaction with the *i*-butane feed was the formation of *n*-butenes and 1,3-butadiene, that is, the skeletal isomerization of the formed *i*-butene (and subsequent dehydrogenation of *n*-butenes). With the *n*-butane feed, the selectivity for isomerization was lower. This is in accordance with the thermodynamics of skeletal isomerization at 580°C. Instead, the main side reactions with the *n*-butane feed were cracking and the formation of heavier compounds. Modification of the catalyst with Mg reduced the selectivity for side reactions.

Butenes can also be formed by oxidative dehydrogenation reaction of butanes to butenes and water without the presence of any gaseous oxygen (11, 43–46). This reaction was likely proceeding under our conditions with the calcined catalysts. We believe that the high proportion of 1,3-butadiene obtained during the first minute on stream in the reaction between *n*-butane and the calcined catalyst was due to oxidative dehydrogenation reaction (47, 48). This would mean that the different acidities of the catalysts had an influence on the distribution of *n*-butenes and 1,3-butadiene as the products of oxidative dehydrogenation as the acidity influenced the selectivity for skeletal isomerization. For all three catalysts, however, the distribution of *n*-butenes and 1,3-butadiene remained very similar after reduction with *n*-butane, CO, and H_2, showing that the influence of the acidity on the distribution of the dehydrogenation products was small. The conversion of *n*-butane to *n*-butenes was not in thermodynamic equilibrium with the VO_x/Al_2O_3 catalysts. Despite this, the distribution of the *n*-butenes and their reaction to 1,3-butadiene was close to the calculated equilibrium value. As well, the dehydrogenation of *i*-butane to *i*-butene was not at equilibrium. The yields of butenes with VO_x catalysts were noticeably better than those obtained with MoO_x catalyst, though they were not yet at the level obtainable with CrO_x catalysts (49).

CONCLUSIONS

Characterization of VO_x/Al_2O_3 catalysts by XPS, ESR, TPR, and FTIR showed that V^{5+} species were reduced to V^{4+} and V^{3+} during reduction with H_2 and CO. The average oxidation state of vanadium obtained with H_2 was slightly lower than obtained with CO. Vanadium was mainly reduced to V^{3+} with H_2, and only a small amount of V^{4+} (B) was measured by ESR. A larger amount of V^{4+} (coordinations A and B) and some V^{3+} were formed during CO reduction. The highest activity in dehydrogenation of butanes to butenes and H_2 was obtained after reduction of the catalysts with CO. It is likely that both V^{4+} and V^{3+} were active species in the dehydrogenation, and, tentatively, we conclude that the activity of V^{4+} (A) was higher than that of V^{3+}.

Modification of the catalyst with Mg caused a decrease in the activity of the catalyst while increasing the selectivity for dehydrogenation. Zr modification caused little change in the activity. The average oxidation state of vanadium and the distribution of oxidation states V^{5+}, V^{4+}, and V^{3+} observed for the three catalysts were similar after reduction of the catalyst with H_2 or CO at 580°C. The oxidation state of vanadium was not, therefore, responsible for the differences in activities. Selectivities for the side reactions of cracking, skeletal isomerization, and coke formation were noticeably different for the V5Zr5 and V5Mg5 catalysts, and the differences were attributed to the acidities of the catalysts.

ACKNOWLEDGMENTS

Support for this research by the EU (Brite Euram) and the Academy of Finland is gratefully acknowledged. We thank Mr. Leif Backman at Helsinki University of Technology for the TPR work; Ms. Heidi Österholm and Mr. Ilkka Savolainen at Fortum Oil and Gas Oy for the XRD analyses and the XPS measurements, respectively; and Mr. V. Keppens of K. U. Leuven for the ESR and DRS measurements.

REFERENCES

1. Weckhuysen, B. M., and Schoonheydt, R. A., *Catal. Today* **51**, 223 (1999).
2. Hakuli, A., Kytökivi, A., and Krause, A. O. I., *Appl. Catal. A: Gen.* **190**, 219 (2000).
3. Buonomo, F., Sanfilippo, D., and Trifirò, F., *in* "Handbook of Heterogeneous Catalysis" (G. Ertl, H. Knözinger, and J. Weitkamp, Eds.), Vol. 5, p. 2140. VCH, Weinheim, 1997.
4. Larese, C., Campos-Martin, J. M., and Fierro, J. L. G., *Langmuir* **16**, 10294 (2000).
5. Harlin, M. E., Backman, L. B., Krause, A. O. I., and Jylhä, O. J. T., *J. Catal.* **183**, 300 (1999).
6. Ledoux, M. J., Meunier, F., Heinrich, B., Pham-Huu, C., Harlin, M. E., and Krause, A. O. I., *Appl. Catal. A: Gen.* **181**, 157 (1999).
7. Harlin, M. E., Krause, A. O. I., Heinrich, B., Pham-Huu, C., and Ledoux, M. J., *Appl. Catal. A: Gen.* **185**, 311 (1999).
8. Johnson, M. M., and Hepp, H. J., U.S. Patent 3 280 210, 1966.
9. Kovach, S. M., and Kmecak, R. A., GB 1 398 531, 1975.
10. Russel, A. S., and Stokes, J. J., *Ind. Eng. Chem.* **38**, 1071 (1946).
11. Harlin, M. E., Niemi, V. M., and Krause, A. O. I., *J. Catal.* **195**, 67 (2000).
12. Niemi, V., internal report, Neste, 1995.
13. Clark, D. M., Tromp, P. J. J., and Arnoldy, P., U.S. Patent 5 220 092, 1993.
14. Lee, F. M., U.S. Patent 4 607 129, 1986.
15. Lee, F. M., U.S. Patent 4 644 089, 1987.
16. Ashmawy, F. M., *J. Appl. Chem. Biotechnol.* **27**, 137 (1977).
17. Eastman, A. D., U.S. Patent 4 327 238, 1982.
18. Eastman, A. D., U.S. Patent 4 371 730, 1983.
19. Martin, G. R., U.S. Patent 3 793 392, 1974.
20. Barri, S. A., Dave, D., and Young, D., Eur. Patent 150 107, 1985.

21. Blasco, T., and López Nieto, J. M., *Appl. Catal. A: Gen.* **157**, 117 (1997).
22. Mamedov, E. A., and Cortés Corberán, V., *Appl. Catal. A: Gen.* **127**, 1 (1995).
23. Cavani, F., and Trifirò, F., *Catal. Today* **51**, 561 (1999).
24. Albonetti, S., Cavani, F., and Trifiró, F., *Catal. Rev. Sci. Eng.* **38**, 413 (1996).
25. Bañares, M. A., Martínez-Huerta, M. V., Gao, X., Fierro, J. L. G., and Wachs, I. E., *Catal. Today* **61**, 295 (2000).
26. Blasco, T., Galli, A., López Nieto, J. M., and Trifiró, F., *J. Catal.* **169**, 203 (1997).
27. Eon, J. G., Olier, R., and Volta, J. C., *J. Catal.* **145**, 318 (1994).
28. Bañares, M., *Catal. Today* **51**, 319 (1999).
29. Kung, H. H., and Kung, M. C., *Appl. Catal. A: Gen.* **157**, 105 (1997).
30. Hakuli, A., Kytökivi, A., Lakomaa, E.-L., and Krause, A. O. I., *Anal. Chem.* **67**, 1881 (1995).
31. Corma, A., López Nieto, J. M., and Paredes, N., *Appl. Catal. A: Gen.* **104**, 161 (1993).
32. Siew Hev Sam, D., Soenen, V., and Volta, J. C., *J. Catal.* **123**, 417 (1990).
33. Gao, X., Ruiz, P., Xin, Q., Guo, X., and Delmon, B., *J. Catal.* **148**, 56 (1994).
34. Khodakov, A., Yang, J., Su, S., Iglesia, E., and Bell, A., *J. Catal.* **177**, 343 (1998).
35. Catana, G., Rao, R. R., Weckhuysen, B. M., Van Der Voort, P., Vansant, E., and Schoonheydt, R. A., *J. Phys. Chem. B* **102**, 8005 (1998).
36. Wachs, I. E., and Weckhuysen, B. M., *Appl. Catal. A: Gen.* **157**, 67 (1997).
37. Ruitenbeek, M., Ph.D. thesis, Utrecht University, The Netherlands, 1999.
38. Eberhardt, M. A., Proctor, A., Houalla, M., and Hercules, D. M., *J. Catal.* **160**, 27 (1996).
39. Chaar, M. A., Patel, D., Kung, M. C., and Kung, H. H., *J. Catal.* **105**, 483 (1987).
40. Blasco, T., López Nieto, J. M., Dejoz, A., and Vázquez, M. I., *J. Catal.* **157**, 271 (1995).
41. Kazansky, V. B., *in* "Handbook of Heterogeneous Catalysis" (G. Ertl, H. Knözinger, and J. Weitkamp, Eds.), Vol. 2, p. 750. VCH, Weinheim, 1997.
42. Busca, G., Finocchio, E., Ramis, G., and Ricchiardi, G., *Catal. Today* **32**, 133 (1996).
43. Pantazidis, A., Bucholz, S. A., Zanthoff, H. W., Schuurman, Y., and Mirodatos, C., *Catal. Today* **40**, 207 (1998).
44. Creaser, D., Andersson, B., Hudgins, R. R., and Silveston, P. L., *J. Catal.* **182**, 264 (1999).
45. Le Bars, J., Auroux, A., Forissier, M., and Vedrine, J. C., *J. Catal.* **162**, 250 (1996).
46. Andersen, P. J., and Kung, H. H., *in* "Studies in Surface Science and Catalysis" (L. Guczi, F. Solymosi, and P. Tétényi, Eds.), Vol. 75, p. 205. Elsevier, Amsterdam/New York, and Akad. Kiadó, Budapest, 1992.
47. Galli, A., López Nieto, J. M., Dejoz, A., and Vazquez, M. I., *Catal. Lett.* **34**, 51 (1995).
48. López Nieto, J. M., Concepción, P., Dejoz, A., Knözinger, H., Melo, F., and Vázquez, M. I., *J. Catal.* **189**, 147 (2000).
49. Harlin, E., Licentiate thesis, Helsinki University of Technology, Finland, 1999.